

ARTICLE OPEN



Heuristic bounds on superconductivity and how to exceed them

Johannes S. Hofmann¹, Debanjan Chowdhury^{2✉}, Steven A. Kivelson³ and Erez Berg¹

What limits the value of the superconducting transition temperature (T_c) is a question of great fundamental and practical importance. Various heuristic upper bounds on T_c have been proposed, expressed as fractions of the Fermi temperature, T_F , the zero-temperature superfluid stiffness, $\rho_s(0)$, or a characteristic Debye frequency, ω_0 . We show that while these bounds are physically motivated and are certainly useful in many relevant situations, none of them serve as a fundamental bound on T_c . To demonstrate this, we provide explicit models where T_c/T_F (with an appropriately defined T_F), $T_c/\rho_s(0)$, and T_c/ω_0 are unbounded.

npj Quantum Materials (2022)7:83; <https://doi.org/10.1038/s41535-022-00491-1>

INTRODUCTION

While superconducting transition temperatures are non-universal properties, and hence not generally amenable to a simple theoretical analysis, understanding what physics determines T_c is of self-evident importance. One approach to this challenge is to focus on a key physical process that contributes to the development of superconducting order, and to formulate an upper bound – either rigorous or heuristic – on T_c ^{1–7}.

In this paper, we examine three proposed bounds on T_c that are expressed as a fraction of a measurable physical quantity of a given system: an appropriately defined Fermi temperature, a characteristic phonon frequency, or the zero-temperature superfluid phase stiffness. While these putative bounds are physically motivated, and provide valuable intuition in many cases of practical importance, we show by explicit counter-examples that they can be violated by an arbitrary amount. In addition to the fundamental importance of these results, we hope they suggest routes to further optimize T_c .

We briefly summarize our key results here:

1. The notion of an upper bound on T_c in terms of an appropriately defined Fermi energy comes from the fact that, in many situations, as $E_F \rightarrow 0$, the electrons have no kinetic energy. Thus, in this limit, the superfluid stiffness must seemingly go to zero. What sets T_c in the limit of small E_F is pertinent to moiré superconductors^{8–13}, where the bands can be tuned to be narrow. To make this question precise, we must define E_F in a strongly interacting system. We propose two such definitions of E_F , in terms of (i) the difference in the chemical potential between a system with a given density of electrons and a system with a vanishing density, or (ii) the energy dispersion of a single electron added to the empty system.

We show that there is no general bound on T_c/E_F by either definition, by studying two explicit models. In the first model, a flat band is separated by an energy gap from a broad band with pair-hopping interaction between the two. The second model consists of a pair of perfectly flat bands with an on-site electron-electron attraction. We show explicitly that the first model violates any putative T_c/E_F bound when using the first definition of E_F above, while the second model violates the

bound using either definition of E_F . Both models have been defined on a two-dimensional lattice for convenience, but generalized versions of the same models in any $D > 1$ can be easily seen to exhibit qualitatively similar behaviors. In the context of two-dimensional systems, we identify T_c as the Berezinskii–Kosterlitz–Thouless (BKT) transition temperature. In contrast with some earlier discussions¹⁴ of this topic, the topology of the flat band plays no essential role in our analysis. Specifically, in our second model, it is the non-zero spatial extent of the Wannier functions rather than any topological property that is the essential feature responsible for the non-vanishing T_c .

2. In two-dimensional systems where T_c is limited by phase fluctuations, an intuitive bound on T_c is given in terms of the zero-temperature phase stiffness, $\rho_s(0)$. This comes from the relation¹⁵ $T_c = \pi\rho_s(T_c^-)/2$, and the (often physically reasonable) assumption that $\rho_s(T)$ is a decreasing function of T , and hence $\rho_s(0) \geq \rho_s(T)$.

We construct an explicit counter-example in a two-band model of bosons (or, equivalently, tightly bound Cooper pairs), where $\rho_s(0)$ can be made arbitrarily smaller than T_c . In this model, $\rho_s(0)$ can even vanish while $T_c > 0$, implying that there is a reentrant transition into the non-superconducting state below T_c .

3. In electron-phonon superconductors, a heuristic bound on T_c/ω_0 (ω_0 being the characteristic phonon frequency) was proposed^{6,7,16}. The reasoning behind this bound is that, as the dimensionless electron-phonon coupling constant λ increases past an $O(1)$ value, the system tends to become unstable, either towards the formation of localized bipolarons or towards a charge density wave state. At the same time (and relatedly), the phonon frequency is renormalized downward as λ increases, suppressing T_c .

Here, we construct an explicit d –dimensional model where these strong-coupling instabilities are avoided, and T_c increases without bound upon increasing λ . The model includes N electronic bands interacting with N^2 phonon modes. The model is solvable asymptotically in the large- N limit; then, the famous Allen-Dynes result¹⁷ $T_c \propto \omega_0\sqrt{\lambda}$ is valid for large λ , so long as $\lambda \ll N$, and hence T_c/ω_0 is unbounded as

¹Department of Condensed Matter Physics, Weizmann Institute of Science, Rehovot 76100, Israel. ²Department of Physics, Cornell University, Ithaca, NY 14853, USA. ³Department of Physics, Stanford University, Stanford, CA 94305, USA. ✉email: debanjanchowdhury@cornell.edu

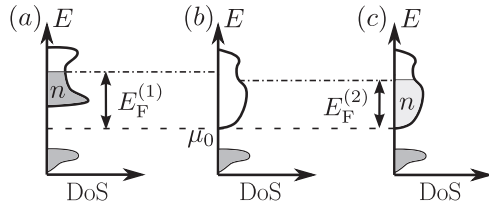


Fig. 1 Illustration of the two operational definitions of E_F . **a**, **b** $E_F^{(1)}$ is defined in Eq. (1) as the difference between the chemical potential at density n (panel a) and the limiting value of the chemical potential μ_0 at which n approaches the value, n_0 , it takes in a reference insulating state (panel b). **c** $E_F^{(2)}$ is defined by Eq. (2) in terms of the density of states $\rho(\epsilon)$ of a single electron excitation added to the reference insulating state.

$N \rightarrow \infty$. Note that at the heuristic level, it is difficult to identify physical circumstances where more than a few phonons are comparably strongly coupled to the relevant electrons. Nevertheless, our analysis suggests that generically, the larger the number of phonon modes coupled to the electrons, the larger the λ at which the suppression of T_c onsets.

RESULTS

Flat band superconductivity: bound on T_c/T_F ?

In most conventional superconductors, T_c is determined by the energy scale associated with electron pairing. On the other hand, across numerous unconventional superconductors, T_c is more strongly sensitive to the ‘phase ordering scale’⁴. In this context, an important recent advance is the result by Hazra, Verma, and Randeria (HVR)⁵ of a rigorous upper bound on $\rho_s(T)$, the temperature-dependent superfluid phase stiffness, in terms of the integral of the optical conductivity over frequency (the optical sum rule). However, since this integral includes all the bands, this upper bound is often of the order of several electron-volts in electronic systems of interest.

At the heuristic level, this bound has been interpreted¹⁸ as implying a bound on T_c/T_F , where $T_F = E_F/k_B$ is the Fermi energy in units of temperature. For a Galilean invariant system with a parabolic band, HVR express their bound in terms of the Fermi energy.

At the outset, it is important to define sharply what we mean by E_F . A particular protocol that is often adopted in experiments to estimate E_F is to use an effective mass, m^* , obtained from quantum oscillations along with an estimate of the Fermi momentum (k_F) from a measurement of the the carrier density n , and then defining $E_F = k_F^2/(2m^*)$; in two dimension, this is equivalent to determining $E_F = \pi\hbar^2 n/m^*$ ¹⁸. This procedure is only possible when there is a nearby Fermi liquid-like state that displays quantum oscillations.

Below, we propose two different definitions of E_F , that we can use in settings that do not rely on any underlying assumptions (e.g., that there is a nearby Fermi liquid) and are also amenable to an experimental interpretation. We consider the case in which we add a given density, n , of electrons to an insulating reference state. We can define E_F as follows:

- Starting from our reference state, we set the temperature to zero and consider the change in the chemical potential, $\mu(n, T=0)$, as we fill in n electrons,

$$E_F^{(1)} \equiv \mu(n, T=0) - \mu_0, \quad (1)$$

as an effective definition of E_F . Here $\mu_0 = \lim_{n \rightarrow 0} \mu(n, T=0)$. Note that the above definition of E_F includes all many-body corrections, which can furthermore be dependent on the density itself, and does not make any reference to any non-interacting limit; see Fig. 1a, b.

- Alternatively, we can define the Fermi energy through the ‘non-interacting’ density of states, $\rho(\epsilon)$, for adding a single electron to the insulating system. This density of states is typically not the same as the one measured at the ‘target’ filling. Here, the Fermi energy ($E_F^{(2)}$) is defined implicitly from the expression

$$n = \int_{\epsilon_{\min}}^{\epsilon_{\min} + E_F^{(2)}} d\epsilon \rho(\epsilon), \quad (2)$$

where ϵ_{\min} is the energy of the ground state with one electron added on top to the insulating reference state; see Fig. 1b, c. $E_F^{(2)}$ is accessible directly in e.g. STM measurements¹⁹. We note that $E_F^{(2)}$ is identical to $E_F^{(1)}$ for non-interacting systems.

Below, we provide model Hamiltonians of interacting electrons in flat bands where the superconducting T_c exceeds the Fermi energy by one or both of the above definitions. Thus, these models exemplify flat band superconductivity, where T_c is determined entirely by the interaction scale^{20–22}. Analogous phenomena may also occur in semi-metals^{23,24}.

Flat band superconductivity induced by a nearby dispersive band: We consider a model consisting of a nearly-flat band and a dispersive band. A closely related model²⁵ has recently been studied in the context of superconductivity in twisted bilayer graphene. The single-particle part of the Hamiltonian is given by

$$H_0 = \sum_{\mathbf{k}, \ell, \sigma} \epsilon_{\ell}(\mathbf{k}) c_{\mathbf{k}, \ell, \sigma}^{\dagger} c_{\mathbf{k}, \ell, \sigma}, \quad (3)$$

where $c_{\mathbf{k}, \ell, \sigma}^{\dagger}$ creates an electron with quasi-momentum \mathbf{k} in band $\ell = 1, 2$ and spin polarization σ . We consider the lower band ($\ell = 1$) to be a flat band with bandwidth, W_1 , that we will ultimately take to be parametrically small (i.e. $W_1 \rightarrow 0$). The upper band ($\ell = 2$) is separated from the flat band by an energy gap, Δ_{gap} , and has a large bandwidth, $W_2 \gg W_1$. The bands are topologically trivial and the Wannier functions are tightly localized on the lattice sites.

We now introduce an on-site interaction which scatters a pair of electrons between the flat band and the dispersive band:

$$H_{\text{int}} = V \sum_{\mathbf{R}} \left[\varphi_{\uparrow}^{\dagger}(\mathbf{R}) \varphi_2(\mathbf{R}) + \text{h.c.} \right], \quad (4)$$

$$\varphi_{\ell}(\mathbf{R}) = c_{\mathbf{R}, \ell, \downarrow} c_{\mathbf{R}, \ell, \uparrow}, \quad (5)$$

where \mathbf{R} labels a lattice site. Let us focus on the case where the flat band is half filled, such that the number of particles per unit cell is $n = 1$.

We consider the case where $V \ll \Delta_{\text{gap}} \ll W_2$. Within mean-field theory, the superconducting transition temperature is given by (see Supplementary Methods),

$$T_{\text{MF}} \approx \left[\frac{v_2 V^2}{8} \ln \left[\frac{W_2}{\Delta_{\text{gap}}} \right] \right], \quad (6)$$

where we have assumed a constant density of states per unit cell, $v_2 = 1/W_2$, in the dispersive band. The zero-temperature phase stiffness is given by (Supplementary Methods)

$$\rho_s(T=0) \approx \frac{V^2}{8\pi\Delta_{\text{gap}}}. \quad (7)$$

Hence $\rho_s(0) \gg T_{\text{MF}}$, which implies that phase fluctuations are unimportant in determining T_c ⁴, i.e. $T_c \approx T_{\text{MF}}^{(1,2)}$.

We now examine the Fermi energies $E_F^{(1,2)}$ defined in Eqs. (1) and (2) and compare them to T_c . Adding a single particle to the empty system, we find that $E_F^{(2)} \sim W_1 \ll T_c$, and hence $T_c/E_F^{(2)}$ can be made arbitrarily large. $E_F^{(1)}$ is computed in Supplementary Methods by calculating the chemical potentials at $n=1$ and $n \rightarrow 0$. The result is $E_F^{(1)} = 2T_{\text{MF}} \sim T_c$. Hence, in this model, $T_c/E_F^{(1)} = O(1)$. An example of a different model where $T_c/E_F^{(1)}$ is unbounded is presented in the next section.

Flat band superconductivity induced by spatial extent of Wannier functions: We now introduce a different model for superconductivity in a narrow band. The model is defined on a two-dimensional square lattice with two electronic orbitals per unit cell. The Hamiltonian is given by

$$H = H_0 + H_U, \quad (8)$$

$$H_0 = t \sum_{k,y,\gamma} \hat{c}_{k,y}^\dagger (\tau_x \sin a_k + \sigma_z \tau_y \cos a_k - \mu) c_{k,y},$$

$$H_U = -\frac{U}{2} \sum_{\mathbf{r},\ell} \delta n_{\mathbf{r},\ell}^2 + V \sum_{\langle \mathbf{r},\mathbf{r}' \rangle, \ell} \delta n_{\mathbf{r},\ell} \delta n_{\mathbf{r}',\ell}. \quad (9)$$

Here, $\hat{c}_{\mathbf{k}}^\dagger = (\hat{c}_{\mathbf{k},1,\uparrow}^\dagger, \hat{c}_{\mathbf{k},1,\downarrow}^\dagger, \hat{c}_{\mathbf{k},2,\uparrow}^\dagger, \hat{c}_{\mathbf{k},2,\downarrow}^\dagger)$, where the operator $\hat{c}_{\mathbf{k},\ell,\sigma}^\dagger$ creates an electron with momentum \mathbf{k} in orbital $\ell = 1, 2$ with spin $\sigma = \uparrow, \downarrow$. We denote $\gamma = \{\sigma, \ell\}$. The Pauli matrices $\tau_{x,y,z}$ and $\sigma_{x,y,z}$ act on the orbital and spin degrees of freedom, respectively, and $\delta n_{\mathbf{r},\ell} \equiv \sum_{\sigma} \hat{c}_{\mathbf{r},\ell,\sigma}^\dagger \hat{c}_{\mathbf{r},\ell,\sigma} - 1$ is the number of particles at site \mathbf{r} and orbital ℓ , relative to half filling. $\langle \mathbf{r}, \mathbf{r}' \rangle$ denotes nearest-neighbor sites. The single-particle Hamiltonian H_0 leads to perfectly flat bands with energies $\varepsilon = \pm t$. The function $a_{\mathbf{k}} \equiv \zeta(\cos k_x + \cos k_y)$ controls the spatial extent of the Wannier functions in each band, tuned by the dimensionless parameter ζ . More specifically, the Wannier functions decay exponentially over a distance proportional to ζ . Note that there is no obstruction towards constructing exponentially localized Wannier functions for the above model since the bands are topologically trivial. This can be seen from the fact that the Berry curvature of the bands is identically zero, since H_0 contains only $\tau_{x,y}$ but not τ_z . The strength of on-site attractive Hubbard interaction is denoted $U > 0$, whereas $V > 0$ is a nearest-neighbor repulsion.

We are interested in the limit where $T \ll U, V \ll \Delta_{\text{gap}} (= 2t)$ and $\zeta \ll 1$. An extensive numerical study of the model (9) beyond this parameter regime has been analyzed in a separate publication²⁶. In this limit, we project H_U to the lower eigenband. The projected Hamiltonian is expanded in powers of ζ . The average density is set to quarter filling per unit cell.

For $\zeta = 0$, the problem effectively reduces to a set of decoupled sites with a strong attractive interaction; the resulting ground state manifold is highly degenerate with local ‘Cooper pairs’ but a vanishing phase stiffness. The linear corrections in ζ vanish due to a chiral symmetry and the orbital l independent interaction strength U . At second order in ζ , the projected interaction, H_U , contains nearest-neighbor pair-hopping and density-density interactions:

$$\widetilde{H}_U = - \sum_{\langle \mathbf{r},\mathbf{r}' \rangle} [J_\perp (\hat{\eta}_{\mathbf{r}}^x \hat{\eta}_{\mathbf{r}'}^x + \hat{\eta}_{\mathbf{r}}^y \hat{\eta}_{\mathbf{r}'}^y) + J_z \hat{\eta}_{\mathbf{r}}^z \hat{\eta}_{\mathbf{r}'}^z]. \quad (10)$$

Here, we have also introduced the pseudospin operators $\hat{\eta}_{\mathbf{r}}^a = (\Psi_{\mathbf{r}}^\dagger \eta^a \Psi_{\mathbf{r}}) / 2$, where $\Psi_{\mathbf{r}}^\dagger = (\hat{c}_{\mathbf{r},\uparrow}^\dagger, \hat{c}_{\mathbf{r},\downarrow}^\dagger)$, $\hat{c}_{\mathbf{r},\sigma}^\dagger$ creates an electron with spin σ in a Wannier-orbital localized around site \mathbf{r} in the lower band of H_0 (with $\tau_y = -\sigma$ for $\zeta = 0$), and η^a are Pauli matrices. The J_\perp and J_z terms correspond to hopping and a nearest-neighbor interaction of the Cooper pairs, respectively, and their strengths are $J_\perp = \zeta^2(2U + V)/8$ and $J_z = \zeta^2 U/4 - V(2 + 9\zeta^2/8)$.

For $V = 0$, the system has an emergent $SU(2)$ symmetry that relates the pairing and charge order parameters²⁷. This symmetry is weakly broken by terms of order $(U/t)^2$, not included in Eq. (10). For $0 < V \ll U$, the problem is equivalent to a two-dimensional pseudospin ferromagnet with a weak easy-plane anisotropy. Parameterizing the anisotropy by $\Delta J = J_\perp - J_z$, we can estimate the critical temperature of the BKT transition as²⁸

$$T_c \sim \pi J_\perp / \log(\pi J_\perp / \Delta J). \quad (11)$$

Note that in the limit $\Delta J \rightarrow 0$ we get $T_c \rightarrow 0$, as required by the Mermin-Wagner-Hohenberg theorem.

We now turn to estimating $E_F^{(1,2)}$. Due to the particle-hole symmetry of the effective Hamiltonian in Eq. (10), the chemical potential at $n = 1$ (i.e., $\langle \hat{\eta}_{\mathbf{r}}^z \rangle = 0$) is $\mu(n = 1) = 0$. In the limit $n \rightarrow 0$, the system consists of dilute Cooper pairs. In this limit, the interactions between the Cooper pairs can be neglected, and the chemical potential is equal to half the energy per Cooper pair: $\mu(n \rightarrow 0) = -(J_\perp - J_z) = -\Delta J$. Importantly, for $J_\perp > J_z$, the system does not phase separate at any density. Therefore, $E_F^{(1)} = \mu(n = 1) - \mu(n \rightarrow 0) = \Delta J$. Comparing this to Eq. (11), we find that for $\Delta J \ll J_\perp, T_c \gg E_F^{(1)}$. We remark that the second band of the microscopic model gives rise to perturbative corrections, controlled by U/Δ_{gap} , that are of subleading order for $E_F^{(1)}$, ΔJ and J_\perp (note that $V \neq 0$); hence, the above conclusion is unchanged. Clearly, since the lower band is completely dispersionless, $E_F^{(2)} = 0$. We conclude that T_c can be made arbitrarily larger than the Fermi energy by either of the two definitions of Eqs. (1) and (2).

It is worth noting that, in the parameter regime we are considering, $\rho_s(0) \sim J_\perp \sim \zeta^2 U$. Hence, the delocalization of the Cooper pairs is entirely due to the interactions and the spatial overlap between the Wannier function of the active band, as in refs. 14,29–33. The finite value of $\rho_s(0)$ and the associated lower bound as derived in refs. 14,29–31 is based on the application of BCS mean-field theory. Here, however, for $U \gg V$, we get $\Delta J \ll J_\perp$ and hence $\rho_s(0) \gg T_c$ [see Eq. (11)].

Bound on $T_c/\rho_s(0)$?

In this section, we turn to the question of whether the zero-temperature phase stiffness, $\rho_s(0)$, sets an upper bound on T_c in two dimensions. $\rho_s(0)$ can be extracted directly from a measurement of the London penetration depth ($\lambda_L^2(0) \propto 1/\rho_s(0)$), or from the imaginary part of the low-frequency optical conductivity.

As is well known, in two spatial dimensions, the phase stiffness right below T_c is related to T_c by the inequality $\rho_s(T \rightarrow T_c^-) \geq 2T_c/\pi$. At a continuous BKT transition, $\rho_s(T \rightarrow T_c^-) = 2T_c/\pi$. However, if the transition is first order, ρ_s right below T_c can be larger than the universal BKT value. See, e.g., ref. 34. However, T_c is not directly related to $\rho_s(0)$. On physical grounds, it often makes sense to identify $\rho_s(0)$ with a ‘phase ordering scale’ that sets an upper limit on T_c ⁴. This is justified by the fact that $\rho_s(T)$ is usually a monotonically decreasing function of temperature, i.e. $\rho_s(0) \geq \rho_s(T_c)$, and therefore T_c can be bounded from above by $\rho_s(0)$. In conventional superconductors, $\rho_s(0) \gg T_c$, and T_c is almost entirely determined by the pairing scale. In contrast, in underdoped cuprates, $\rho_s(0)$ is close to T_c , as illustrated by the famous Uemura plot³⁵. This suggests that in these systems, phase fluctuations play an important role in limiting T_c ⁴.

While this line of reasoning is likely correct in most circumstances, we will show here that—as a matter of principle—there is *no* bound on $T_c/\rho_s(0)$. We outline a concrete model where $\rho_s(0)$ can be made arbitrarily smaller than $\rho_s(T_c)$ (Fig. 2).

Let us begin with a two-dimensional lattice model of two species of (complex) bosons, b_1, b_2 ,

$$H^b = H_0^b + H_{\text{int}}^b, \quad (12)$$

$$H_0^b = \sum_{\mathbf{a},\mathbf{k}} \varepsilon_{\mathbf{a}}(\mathbf{k}) b_{\mathbf{a},\mathbf{k}}^\dagger b_{\mathbf{a},\mathbf{k}}, \quad (13)$$

where $\varepsilon_2(\mathbf{k})$ is assumed to have a large bandwidth, W_2 , and $\varepsilon_1 = \varepsilon_2(0) - \varepsilon_0$ forms a completely flat band at an energy ε_0 below the bottom of the ε_2 band, i.e. the b_1 bosons are completely localized on individual sites. The dispersion of the two species of bosons is illustrated in Fig. 2. For the purpose of our discussion here, we can approximate $\varepsilon_2(\mathbf{k}) \approx k^2/2m_b$ near the bottom of the broad band. H_{int}^b includes an on-site (Hubbard) interaction of strength $U_{1,2}$ for the $b_{1,2}$ bosons. We take $U_2 \ll W_2$ whereas $U_1 \rightarrow \infty$, implying that the number of b_1 bosons on each localized site can only be 0 or 1. The total average number of bosons per unit cell is chosen to be $n_b > 1$.

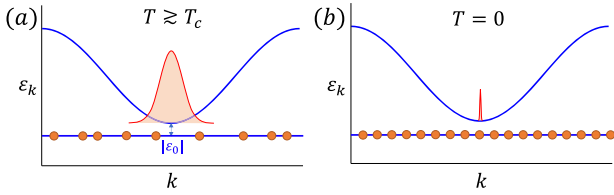


Fig. 2 Schematic illustration of the dispersion and momentum distribution function of the bosons in the model with unbounded $T_c/\rho_s(0)$ [Eq. (12)]. **a** At $T \gtrsim T_c$ the flat band is approximately half filled, and the remaining $n_b - 1/2$ bosonic particles per site occupy the dispersive band. **b** At $T = 0$, the flat band is completely filled with one boson per site, and hence the superfluid density is proportional to $n_b - 1$.

At temperatures near T_c , the chemical potential is slightly above the bottom of the broad band. Then, assuming that $\varepsilon_0 \ll T$, the average occupation of the localized sites is close to $1/2$ (since the b_1 bosons are essentially hard-core bosons at effectively ‘infinite’ temperature), so there are approximately $n_b - 1/2$ bosons per unit cell left to occupy the broad band. The critical temperature is $T_c \sim \frac{n_b - 1/2}{2m_b}$, up to logarithmic corrections in $\frac{n_b - 1/2}{2m_b}/U_2$ ^{36–38}. Since we are in two spatial dimensions, in the absence of interactions, $T_c = 0$. The momentum distribution of particles at $T \gtrsim T_c$ is shown schematically in Fig. 2a.

On the other hand, at $T = 0$, all the localized sites are filled with one boson. The density of bosons in the broad band is thus $n_b - 1$, and the superfluid stiffness is $\rho_s \approx \frac{n_b - 1}{2m_b}$. The boson distribution function is illustrated in Fig. 2b. Clearly, the ratio $T_c/\rho_s(0)$ can be made arbitrary large by letting $n_b \rightarrow 1^+$. If $1/2 < n_b < 1$, the ground state is not a superfluid, and there is a reentrant transition into a superconducting state with increasing T .

Note that in our simple model (Eq. (12)), the numbers of the two boson species are separately conserved. However, we do not expect the key results to be changed qualitatively by the addition of a weak hybridization between the two species, that breaks this separate conservation of the two boson numbers. In particular, a small hybridization generically produces a perturbative correction to T_c and $\rho_s(0)$.

Indeed, a mild version of this sort of breakdown of the heuristic bound on $T_c/\rho_s(0)$ has been documented experimentally in Zn-doped cuprates³⁹. Here, the pristine material comes close to saturating the heuristic bound; light Zn doping suppresses T_c but apparently suppresses $\rho_s(0)$ more rapidly, leading to a ratio that slightly exceeds the value proposed in ref. 4. This was explained—likely correctly—by the authors of ref. 39 as being due to Zn-induced inhomogeneity of the superfluid response. This explanation is spiritually close to the model discussed above: each Zn impurity destroys the superconductor in its vicinity, possibly due to pinning of local spin-density-wave order⁴⁰. In some sense, this can be thought of as a state with localized d-wave pairs near the impurities. This effect depletes the condensate at low temperature, causing a decrease in the superfluid density. However, near T_c , this effect weakens, as the spin-density wave order partially melts. From this perspective, it would be interesting to explore whether this violation can be made parametrically large with increasing Zn concentration - approaching the point at which $T_c \rightarrow 0$.

Electron-phonon superconductivity: bound on T_c/ω_0 ?

Recently, it has been proposed that T_c in an electron-phonon superconductor can never exceed a certain fraction of the characteristic phonon frequency, ω_0 ^{6,7}. This putative bound implies that Migdal–Eliashberg (ME) theory^{41–43} must breakdown when the dimensionless electron-phonon coupling λ is of order unity^{6,16}, since according to ME theory, T_c grows without limit with

increasing λ ¹⁷. In general, the failure of ME theory at $\lambda = O(1)$ is a result of strong-coupling effects: (i) The lattice tends to become unstable for large λ , resulting in a charge density wave (CDW) transition; (ii) electrons become tightly bound into bipolarons, whose kinetic energy is strongly quenched in the strong-coupling limit; and (iii) as λ increases, the phonon frequency renormalizes downward by an appreciable amount, $\Delta\omega$, suppressing T_c ⁴⁴. The softening of ω_0 due to electron-phonon coupling is formally taken into account in Eliashberg theory. Often, however, the phonon spectral function is taken as given or is fit to experiment, as is done in ref. 17.

These strong-coupling effects certainly play an important role in limiting T_c in real systems, where it is typically found never to exceed about $0.1 \omega_0$ across numerous conventional superconductors⁷. Determinant Monte Carlo simulations of the paradigmatic Holstein model reveal that ME theory indeed fails for $\lambda = O(1)$, and the maximal T_c is significantly below ω_0 ⁶. As we shall now show, however, this is not a rigorous bound on T_c .

To demonstrate this, we consider a particular large $-N$ variant of the electron-phonon problem^{45,46} with N -component electrons and $N \times N$ -component (‘matrix’) phonons, defined on a d -dimensional hypercubic lattice. The Hamiltonian is given by

$$H = H_e + H_{\text{ph}} + H_{e-\text{ph}}, \quad (14)$$

$$H_e = \sum_{a=1}^N \sum_{\mathbf{r}, \mathbf{r}', \sigma} (-t_{\mathbf{r}\mathbf{r}'} - \mu \delta_{\mathbf{r}\mathbf{r}'}) c_{\mathbf{r}, \sigma, a}^\dagger c_{\mathbf{r}', \sigma, a}, \quad (15)$$

$$H_{\text{ph}} = \sum_{a, b=1}^N \sum_{\mathbf{r}} \left(\frac{p_{\mathbf{r}, ab}^2}{2M} + \frac{K}{2} X_{\mathbf{r}, ab}^2 \right), \quad (16)$$

$$H_{e-\text{ph}} = \frac{\alpha}{\sqrt{N}} \sum_{a, b=1}^N \sum_{\mathbf{r}, \sigma} X_{\mathbf{r}, ab} c_{\mathbf{r}, \sigma, a}^\dagger c_{\mathbf{r}, \sigma, b}. \quad (17)$$

Here, $c_{\mathbf{r}, \sigma, a}^\dagger$ creates an electron at position \mathbf{r} with spin σ in ‘orbital’ a . The hopping parameters $t_{\mathbf{r}\mathbf{r}'}$ and chemical potential μ are assumed to be identical for all orbitals. We have introduced a real, symmetric matrix of phonon displacements, $\mathbf{X}_{\mathbf{r}}$ and their canonically conjugate momenta, $\mathbf{P}_{\mathbf{r}}$, with frequency $\omega_0 = \sqrt{K/M}$, assumed to be much smaller than the Fermi energy. The phonons are taken to be dispersionless for simplicity. The purely on-site electron-phonon coupling constant is denoted α , with a N -dependent normalization factor that ensures that the model has a finite energy density in the $N \rightarrow \infty$ limit. The dimensionless electron-phonon coupling constant is defined as $\lambda = \alpha^2 v(0)/K$, where $v(0)$ is the electronic density of states at the Fermi level per orbital.

We are interested in the large $-N$ limit of the model defined in Eq. (14). Since the number of phonon degrees of freedom is much larger than the number of electron orbitals, the phonon dynamics are essentially unaffected by the coupling to the electrons, even when the electrons are strongly perturbed. This implies that the strong-coupling effects mentioned above are suppressed, even for $\lambda \gg 1$. In particular, as we show in Supplementary Methods, there is no lattice instability or polaron formation as long as $\lambda \ll N$, and the softening of the phonon frequency is only of the order of $\Delta\omega \sim \lambda\omega_0/N$.

To zeroth order in $1/N$, the equations for the electron self-energy and the pairing vertex are exactly those given by Eliashberg theory, whereas the phonon self-energy is of order $1/N$ (see Fig. 3). Thus, the self-consistent equations for the pairing vertex are identical to those of ME theory neglecting the renormalization of the phonons, and hence the result is the same. In particular, for $1 \ll \lambda \ll N$, $T_c \approx 0.1827 \omega_0 \sqrt{\lambda}$ ¹⁷. Implicit in the fact that Migdal–Eliashberg theory is exact at $N \rightarrow \infty$ is an assurance that there is no suppression of T_c by phase fluctuations. In the $d=2$ version of our model, the BKT temperature differs from

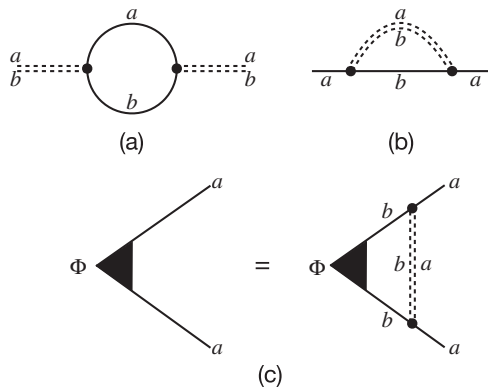


Fig. 3 Diagrams of the large- N expansion for the coupled electron-phonon model. Self-energy for the **a** phonon (X_{ab}), and **b** electron (c_d) fields, respectively. **c** Bethe-Salpeter equation for the pairing vertex, Φ . Double dashed and solid lines represent the phonon and electron fields. Solid circles (triangles) denote the electron-phonon (pairing) vertex.

the mean-field transition temperature only by a $1/N$ correction. More specifically, this follows from the observation that the superfluid stiffness is $\mathcal{O}(N)$. Thus, T_c is unbounded.

The key ingredient in our model that allows us to take $\lambda > 1$ without suffering from lattice instabilities is that the different phonon modes couple to electron bilinears that do not commute with each other [see Eq. (17)]. This limits the energy gain from distorting a given set of phonon modes when forming a CDW or a polaron bound state, since the resulting perturbations to the electronic Hamiltonian cannot be diagonalized simultaneously. In contrast, the contributions of the individual phonon modes add algebraically in the total dimensionless coupling λ that enters the equation for the pairing vertex (the same dimensionless coupling also determines the resistivity in the normal state of this model⁴⁵).

It is worth noting that while these considerations may be of some use in searching for systems with ever higher T_c , as a practical matter it may be difficult to significantly violate the proposed heuristic bound. To achieve $T_c \approx \omega_0$ requires the extremely large value of $\lambda \approx 25$. At the same time, to avoid polaron formation requires $N \gg \lambda$, which means the number of distinctly coupled phonon modes would have to be $N^2 \gg \lambda^2 \sim 625$!

DISCUSSION

The notion of a fundamental upper bound on T_c for models of interacting electrons is an attractive concept. In this paper, we have demonstrated that while there are numerous physical settings where such bounds can be formulated at a heuristic level, there exists no fundamental, universal upper bound on T_c in terms of the characteristic energy scales of interest to us, which include an appropriately defined T_F , $\rho_s(0)$ and ω_0 . We have constructed explicit counter-examples which violate these heuristic bounds by an arbitrary amount.

On the experimental front, it would be fruitful to look for candidate materials where the heuristic bounds are violated by a large amount. The fact that these bounds are usually satisfied is to be expected, since although the bounds are not rigorous, the physical reasoning behind them is quite robust. As our theoretical discussion illustrates, whenever such bounds are violated, there is an interesting underlying physical reason behind the violation; moreover, the mechanisms behind the violation of the heuristic bounds may suggest ways to optimize T_c . Our work provides two such examples. Flat band systems with a large spatial extent of the Wannier functions are a promising platform for increasing T_c . In electron-phonon systems, the instabilities that limit T_c at large electron-phonon interaction strength can be partially mitigated if

the coupling is shared between several active phonon modes that couple to non-commuting electronic operators.

METHODS

All analytical calculations are explicit presented in Supplementary Information.

Received: 3 June 2021; Accepted: 31 July 2022;

Published online: 29 August 2022

REFERENCES

- McMillan, W. L. Transition temperature of strong-coupled superconductors. *Phys. Rev.* **167**, 331–344 (1968).
- Cohen, M. L. & Anderson, P. W. Comments on the maximum superconducting transition temperature. *AIP Conf. Proc.* **4**, 17–27 (1972).
- Ginzburg, V. L. High-temperature superconductivity (history and general review). *Sov. Phys. Usp.* **34**, 283–288 (1991).
- Emery, V. J. & Kivelson, S. A. Importance of phase fluctuations in superconductors with small superfluid density. *Nature* **374**, 434–437 (1995).
- Hazra, T., Verma, N. & Randeria, M. Bounds on the superconducting transition temperature: applications to twisted bilayer graphene and cold atoms. *Phys. Rev. X* **9**, 031049 (2019).
- Esterlis, I. et al. Breakdown of the Migdal-Eliashberg theory: a determinant quantum Monte Carlo study. *Phys. Rev. B* **97**, 140501 (2018).
- Esterlis, I., Kivelson, S. A. & Scalapino, D. J. A bound on the superconducting transition temperature. *npj Quant. Mater.* **3**, 59 (2018).
- Cao, Y. et al. Unconventional superconductivity in magic-angle graphene superlattices. *Nature* **556**, 43–50 (2018).
- Yankowitz, M. et al. Tuning superconductivity in twisted bilayer graphene. *Science* **363**, 1059–1064 (2019).
- Lu, X. et al. Superconductors, orbital magnets and correlated states in magic-angle bilayer graphene. *Nature* **574**, 653–657 (2019).
- Arora, H. S. et al. Superconductivity in metallic twisted bilayer graphene stabilized by WSe₂. *Nature* **583**, 379–384 (2020).
- Park, J. M., Cao, Y., Watanabe, K., Taniguchi, T. & Jarillo-Herrero, P. Tunable strongly coupled superconductivity in magic-angle twisted trilayer graphene. *Nature* **590**, 249–255 (2021).
- Hao, Z. et al. Electric field tunable superconductivity in alternating-twist magic-angle trilayer graphene. *Science* **371**, 1133–1138 (2021).
- Xie, F., Song, Z., Lian, B. & Bernevig, B. A. Topology-bounded superfluid weight in twisted bilayer graphene. *Phys. Rev. Lett.* **124**, 167002 (2020).
- Nelson, D. R. & Kosterlitz, J. M. Universal jump in the superfluid density of two-dimensional superfluids. *Phys. Rev. Lett.* **39**, 1201–1205 (1977).
- Chubukov, A. V., Abanov, A., Esterlis, I. & Kivelson, S. A. Eliashberg theory of phonon-mediated superconductivity—When it is valid and how it breaks down. *Ann. Phys.* **417**, 168190 (2020).
- Allen, P. B. & Dynes, R. C. Transition temperature of strong-coupled superconductors reanalyzed. *Phys. Rev. B* **12**, 905–922 (1975).
- Park, J. M., Cao, Y., Watanabe, K., Taniguchi, T. & Jarillo-Herrero, P. Tunable strongly coupled superconductivity in magic-angle twisted trilayer graphene. *Nature* **590**, 249–255 (2021).
- Xie, Y. et al. Spectroscopic signatures of many-body correlations in magic-angle twisted bilayer graphene. *Nature* **572**, 101–105 (2019).
- Khodel', V. A. & Shaginyan, V. R. Superfluidity in system with fermion condensate. *Sov. Phys. JETP Lett.* **51**, 553–555 (1990).
- Heikkilä, T. T., Kopnin, N. B. & Volovik, G. E. Flat bands in topological media. *Sov. Phys. JETP Lett.* **94**, 233–239 (2011).
- Volovik, G. E. Flat band in topological matter. *J. Supercond. Nov. Magn.* **26**, 2887–2890 (2013).
- Kopnin, N. B. & Sonin, E. B. BCS superconductivity of Dirac electrons in graphene layers. *Phys. Rev. Lett.* **100**, 246808 (2008).
- Kopnin, N. B. & Sonin, E. B. Supercurrent in superconducting graphene. *Phys. Rev. B* **82**, 014516 (2010).
- Dong, Z. & Levitov, L. Activating superconductivity in a repulsive system by high-energy degrees of freedom. Preprint at <https://arxiv.org/abs/2103.08767> (2021).
- Hofmann, J. S., Berg, E. & Chowdhury, D. Superconductivity, charge density wave, and supersolidity in flat bands with tunable quantum metric. Preprint at <https://arxiv.org/abs/2204.02994> (2022).
- Tovmasyan, M., Peotta, S., Liang, L., Törmä, P. & Huber, S. D. Preformed pairs in flat Bloch bands. *Phys. Rev. B* **98**, 134513 (2018).
- Nelson, D. R. & Pelcovits, R. A. Momentum-shell recursion relations, anisotropic spins, and liquid crystals in $2 + \epsilon$ dimensions. *Phys. Rev. B* **16**, 2191–2199 (1977).

29. Peotta, S. & Törmä, P. Superfluidity in topologically nontrivial flat bands. *Nat. Commun.* **6**, 8944 (2015).
30. Hu, X., Hyart, T., Pikulin, D. I. & Rossi, E. Geometric and conventional contribution to the superfluid weight in twisted bilayer graphene. *Phys. Rev. Lett.* **123**, 237002 (2019).
31. Julku, A., Peltonen, T. J., Liang, L., Heikkilä, T. T. & Törmä, P. Superfluid weight and Berezinskii-Kosterlitz-Thouless transition temperature of twisted bilayer graphene. *Phys. Rev. B* **101**, 060505 (2020).
32. Hofmann, J. S., Berg, E. & Chowdhury, D. Superconductivity, pseudogap, and phase separation in topological flat bands. *Phys. Rev. B* **102**, 201112 (2020).
33. Verma, N., Hazra, T. & Randeria, M. Optical spectral weight, phase stiffness, and T_c bounds for trivial and topological flat band superconductors. *PNAS* **118**, e2106744118 (2021).
34. Domany, E., Schick, M. & Swendsen, R. H. First-order transition in an xy model with nearest-neighbor interactions. *Phys. Rev. Lett.* **52**, 1535–1538 (1984).
35. Uemura, Y. J. et al. Universal correlations between T_c and $\frac{\rho_s}{m^*}$ (carrier density over effective mass) in high- T_c cuprate superconductors. *Phys. Rev. Lett.* **62**, 2317–2320 (1989).
36. Popov, V. N. On the theory of the superfluidity of two-and one-dimensional Bose systems. *Theor. Math. Phys.* **11**, 354–365 (1972).
37. Kagan, Y., Svistunov, B. & Shlyapnikov, G. Influence on inelastic processes of the phase transition in a weakly collisional two-dimensional Bose gas. *Sov. Phys. JETP* **66**, 314–323 (1987).
38. Fisher, D. S. & Hohenberg, P. C. Dilute Bose gas in two dimensions. *Phys. Rev. B* **37**, 4936–4943 (1988).
39. Nachumi, B. et al. Muon spin relaxation studies of Zn-substitution effects in high- T_c cuprate superconductors. *Phys. Rev. Lett.* **77**, 5421–5424 (1996).
40. Hirota, K., Yamada, K., Tanaka, I. & Kojima, H. Quasi-elastic incommensurate peaks in $\text{La}_{2-x}\text{Sr}_x\text{Cu}_{1-y}\text{Zn}_y\text{O}_{4-\delta}$. *Phys. B Condens. Matter* **241**, 817–819 (1997).
41. Migdal, A. Interaction between electrons and lattice vibrations in a normal metal. *Sov. Phys. JETP* **7**, 996–1001 (1958).
42. Eliashberg, G. Interactions between electrons and lattice vibrations in a superconductor. *Sov. Phys. JETP* **11**, 696–702 (1960).
43. Marsiglio, F. & Carbotte, J. P. *Electron-Phonon Superconductivity*, 73–162 (Springer Berlin Heidelberg, Berlin, Heidelberg, 2008).
44. Moussa, J. E. & Cohen, M. L. Two bounds on the maximum phonon-mediated superconducting transition temperature. *Phys. Rev. B* **74**, 094520 (2006).
45. Werman, Y. & Berg, E. Mott-Ioffe-Regel limit and resistivity crossover in a tractable electron-phonon model. *Phys. Rev. B* **93**, 075109 (2016).
46. Werman, Y., Kivelson, S. A. & Berg, E. Non-quasiparticle transport and resistivity saturation: a view from the large- n limit. *npj Quant. Mater.* **2**, 7 (2017).

ACKNOWLEDGEMENTS

We thank Pablo Jarillo-Herrero, Mohit Randeria, and J.M. Tranquada for stimulating discussions. S.A.K. was supported, in part, by the National Science Foundation (NSF)

under Grant No. DMR2000987. D.C. was supported by the faculty startup grants at Cornell University. E.B. and J.H. were supported by the European Research Council (ERC) under grant HQMAT (Grant Agreement No. 817799), the Israel-US Binational Science Foundation (BSF), and by a Research grant from Irving and Cherna Moskowitz.

AUTHOR CONTRIBUTIONS

All authors contributed to the research and wrote the manuscript.

COMPETING INTERESTS

The authors declare no competing interests.

ADDITIONAL INFORMATION

Supplementary information The online version contains supplementary material available at <https://doi.org/10.1038/s41535-022-00491-1>.

Correspondence and requests for materials should be addressed to Debanjan Chowdhury.

Reprints and permission information is available at <http://www.nature.com/reprints>

Publisher's note Springer Nature remains neutral with regard to jurisdictional claims in published maps and institutional affiliations.



Open Access This article is licensed under a Creative Commons Attribution 4.0 International License, which permits use, sharing, adaptation, distribution and reproduction in any medium or format, as long as you give appropriate credit to the original author(s) and the source, provide a link to the Creative Commons license, and indicate if changes were made. The images or other third party material in this article are included in the article's Creative Commons license, unless indicated otherwise in a credit line to the material. If material is not included in the article's Creative Commons license and your intended use is not permitted by statutory regulation or exceeds the permitted use, you will need to obtain permission directly from the copyright holder. To view a copy of this license, visit <http://creativecommons.org/licenses/by/4.0/>.

© The Author(s) 2022